

Searching for GeV-scale Majorana Dark Matter: inter spem et metum

ADIL JUEID^{1,*} and SALAH NASRI^{2,3,†}

¹*Department of Physics, Konkuk University, Seoul 05029, Republic of Korea*

²*Department of physics, United Arab Emirates University, Al-Ain, UAE.*

³*The Abdus Salam International Centre for Theoretical Physics, Strada Costiera 11, I-34014, Trieste, Italy.*

We suggest a minimal model for GeV scale Majorana dark matter (DM) coupled to the standard model lepton sector via a charged scalar singlet. We show that there is anti-correlation between the spin-independent DM-Nucleus scattering cross section (σ_{SI}) and the DM relic density. Moreover, we find that even when DM couplings are of order unity, σ_{SI} is below the current experimental bound but above the neutrino floor, which makes it testable in future DM direct detection experiments. Furthermore, the model can be probed exclusively at high energy lepton colliders with the smoking guns are the mono-Higgs production and same sign charged Higgs pair production.

The existence of dark Matter (DM) in the universe is an established fact supported by various observations at the sub-galactic, galactic, and cosmological scales (for a review, see e.g. [1]). The measurements of CMB anisotropies implied that DM constitutes about 80% of the matter budget in the universe with density of $\Omega_{DM}h^2 = 0.1198 \pm 0.0015$ [2] and standard theories of structure formation requires it to be non-relativistic when gravitational clustering started at the matter-radiation equality. This type of DM is known as cold DM (CDM). One of the simplest scenarios of CDM is the thermal-freeze out mechanism in which the DM can be accommodated by Weakly Interacting Massive Particles (WIMPs) produced in thermal bath and as the universe expands and cools down their relic abundance freeze-out when temperature drops below their mass. Possible evidence for WIMP DM has driven numerous experimental efforts to search for it via direct detection [3, 4], indirect detection [5–8] and in collider experiments [9, 10]. Unfortunately, no signal for CDM has been detected and stringent limit on the cross section of their scattering off nucleus in the mass range GeV to TeV are obtained. Moreover, a model-independent estimates of the limits on the annihilation cross sections of WIMP DM imply strong constraints on models with s -wave annihilation channel [11]. These strong exclusions combined with the null results from direct detection experiments put an end to the most minimal model for GeV-scale DM candidate, i.e. the SM with real scalar singlet [12, 13] which called for several extensions [14, 15].

Models with a singlet Majorana fermion as a DM candidate can potentially avoid these constraints due to the fact that their annihilation is dominated by p -wave amplitudes in addition of being both minimal and predictive. On the other hand, the scattering cross section of the Majorana DM off the nucleus is induced at the one-loop order because of the absence of tree level couplings of the Majorana DM to the Z/H bosons. Consequently, models containing Majorana DM can evade easily direct detection constraints even for model parameters of order $\mathcal{O}(1)$ and thus avoiding the over-abundance condition

$\Omega_{WIMP}h^2 \leq \Omega_{Planck}h^2$. Models containing Majorana DM are phenomenologically very attractive as they can easily address the question of the smallness of neutrino mass through radiative mass generation mechanism [16, 17], and the question of baryon asymmetry in the universe through electroweak baryogenesis [18]. In this Letter, we suggest a very simple model which extends the Standard Model (SM) particle content by two gauge singlets: a charged scalar and a Majorana fermion. Using simple correlations between the relic abundance and the predicted spin-independent cross section, we show that the model is neither excluded nor close to the neutrino-floor region. On the other hand, we find that the model can be exclusively probed at lepton colliders such as the International Linear Collider (ILC), and we study its potential discovery through both the electron-electron and the electron-positron options.

We consider a minimal extension of the SM which contains, in addition to the SM particle content, two gauge-singlet fields; a charged scalar S and a right handed (RH) neutral fermion N . In this simplified model, the RH fermion plays the role of the DM candidate while the charged scalar is a mediator of the DM-visible interaction. To ensure the stability of DM in the universe, we impose an exact discrete symmetry Z_2 under which all the SM fields are even while the new states are odd, i.e. $\{V^\mu, \Phi, \ell, q\} \rightarrow \{V^\mu, \Phi, \ell, q\}$, and $\{S, N\} \rightarrow \{-S, -N\}$. Under these symmetry requirements, the most general Yukawa Lagrangian can be written as

$$\mathcal{L}_{Yuk} \supset \sum_{\ell=e,\mu,\tau} y_\ell \bar{\ell}_R^c S N_R + \frac{1}{2} M_N \bar{N}_R (N_R)^c + h.c. \quad (1)$$

The most general CP-invariant, and dimension four potential involving the SM Higgs doublet Φ and the charged Higgs scalar S can be written as

$$V(\Phi, S) = -m_{11}^2 |\Phi|^2 + m_{22}^2 |S^\dagger S| + \lambda_1 |\Phi|^4 + \lambda_2 |S^\dagger S|^2 + \lambda_3 |\Phi|^2 |S^\dagger S|^2, \quad (2)$$

with $m_{11}^2, m_{22}^2, \lambda_{i,i=1,2,3}$ are real parameters. After electroweak symmetry breaking, one lefts with a CP-even

scalar H which is identified with the recently discovered 125 GeV SM Higgs boson and a pair of charged scalars H^\pm . Their tree-level masses are given by: $m_H^2 = \lambda_1 v^2$ and $m_{H^\pm}^2 = m_{22}^2 + \frac{1}{2}\lambda_3 v^2$. In addition to the SM parameters, this simple model contains seven independent parameters which we choose as: $\{m_{H^\pm}, m_N, \lambda_2, \lambda_3, y_e, y_\mu, y_\tau\}$. For convenience, we define y_N as the combination of the new Yukawa couplings as $y_N = \sqrt{y_e^2 + y_\mu^2 + y_\tau^2}$. The parameters of the model are subject to various theoretical and experimental constraints. Owing to the fact that the charged Higgs state is gauge singlet, constraints from direct LHC searches and from electroweak precision measurements do not apply in our model. On the other hand, the SM Higgs boson is really SM-like, i.e. there is no modification of tree-level Higgs couplings to fermions and gauge bosons. Therefore, the only modification to Higgs boson decay rates comes from the effect of the charged Higgs boson on the one-loop induced $H \rightarrow \gamma\gamma$ decay width [19]. In this work, we use the ATLAS-CMS combined measurement of $|\kappa_\gamma| = \sqrt{\Gamma(H \rightarrow \gamma\gamma)/\Gamma(H \rightarrow \gamma\gamma)_{\text{SM}}} = 0.87^{+0.14}_{-0.09}$ [20].

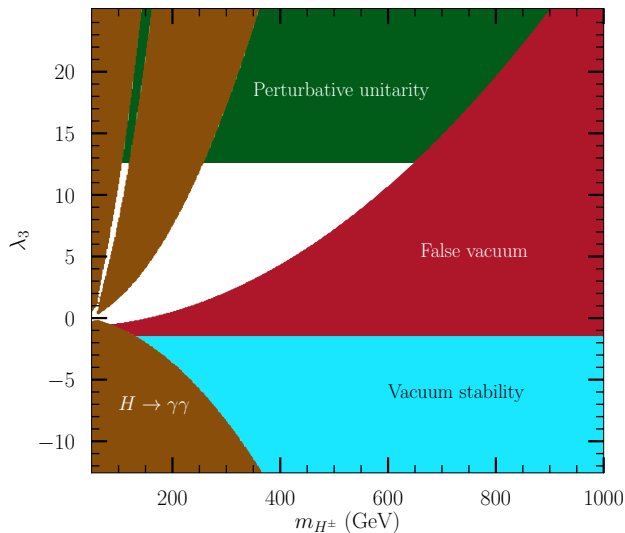


FIG. 1. Summary of the impact of theoretical and experimental constraints on the parameter space of the scalar sector of the model. The constraints are depicted in the mass of the charged Higgs boson m_{H^\pm} and λ_3 for $\lambda_2 = 2$. The excluded regions from Higgs boson decay to photons (brown), from vacuum stability (cyan), from false vacuum (red), and from perturbative unitarity (green). The white shaded area corresponds to the allowed region of the 2D parameter space.

This model is subject to a number of theoretical constraints such as the boundness-from-below requirements (vacuum stability) [21], perturbative unitarity [22], and that the vacuum of the inert scalar should be a global minimum [23]. A summary of the theoretical and experimental constraints are shown in Fig. 1. The combina-

tion of all these constraints restricts the allowed range of the Charged Higgs boson mass to be below 400 GeV for $\lambda_3 \simeq 4$. The constraints on the Yukawa coupling y_N mainly come from the limit on Higgs boson invisible decay branching fraction; $\text{BR}(H \rightarrow \text{invisible}) \equiv B_{\text{inv}}$. In this model, the Higgs invisible proceeds at the one-loop order which we have computed using FEYNARTS, FORMCALC and LOOPTOOLS [24, 25]. The strongest and up-to-date constraint on B_{inv} was reported on by the CMS collaboration from a combination of the search results carried at $7\oplus 8\oplus 13$ TeV; they found $B_{\text{inv}} < B_{\text{upper}} = 0.19$ at 95% CL [26] assuming SM production rates of the Higgs boson. Using the results of these searches, we derive an upper bound on the magnitude of y_N

$$y_N < \left(\frac{2048\pi^5 \Gamma_H^{\text{SM}}}{\beta_N^{3/2} m_H \lambda_3^2 v^2 m_N^2 |C_0 + C_2|^2 \left(\frac{1}{B_{\text{upper}}} - 1 \right)} \right)^{1/4} \quad (3)$$

with $\beta_N = (1 - 4m_N^2/m_H^2)$, and $C_{0,2} \equiv C_{0,2}(m_N^2, m_H^2, m_N^2, m_\ell^2, m_{H^\pm}^2, m_{H^\pm}^2)$ are the Passarino-Veltman functions [27]. For instance, for $m_N \simeq 40$ GeV, $\lambda_3 = 4$ and $m_{H^\pm} = 250$ (400) GeV, we get $y_N < 2.5$ (4.1).

Constraints from lepton-flavor violating decays on the y_ℓ couplings are extremely important as we will see. The most stringent bound comes from the branching ratio of $\mu \rightarrow e\gamma$ decay. We obtain

$$\begin{aligned} y_e y_\mu &< \left(\frac{2.855 \times 10^{-5}}{\text{GeV}} \right)^2 \frac{m_{H^\pm}^2}{|\mathcal{F}(m_N^2/m_{H^\pm}^2)|}, \\ y_e y_\tau &< \left(\frac{4.428 \times 10^{-4}}{\text{GeV}} \right)^2 \frac{m_{H^\pm}^2}{|\mathcal{F}(m_N^2/m_{H^\pm}^2)|}, \\ y_\tau y_\mu &< \left(\frac{4.759 \times 10^{-4}}{\text{GeV}} \right)^2 \frac{m_{H^\pm}^2}{|\mathcal{F}(m_N^2/m_{H^\pm}^2)|}, \end{aligned} \quad (4)$$

where we have used the up-to date bounds from the MEG [28] and BABAR [29] experiments, and $\mathcal{F}(X)$ is the loop-function which can be found in [30, 31]. The implications of these constraints on the product of the couplings are very important. For example, if we fix $y_e = 2$, we found that $\{y_e y_\mu, y_\tau y_e, y_\tau y_\mu\} < \{1.5-6.7 \times 10^{-4}, 0.05-0.1, 0.20-1.82 \times 10^{-5}\}$ if we vary the charged Higgs mass in the range [250, 400] GeV.¹

The main contribution to the relic density of the N particles comes from their annihilation into charged leptons via the exchange of a charged scalar in the t - and

¹ Different scenarios where we can have $y_e \simeq y_\mu \simeq y_\tau \simeq 10^{-3}$ or $y_\tau \simeq y_\mu \gg y_e \simeq 10^{-4}$ are possible as well, but none of these scenarios are phenomenologically plausible since the production rates at lepton colliders will be extremely small – the cross sections depend exclusively on y_e . Theoretically, it could be possible to have a discrete flavor symmetry which allows for $y_e \simeq \mathcal{O}(1) \gg y_\tau \gg y_\mu$.

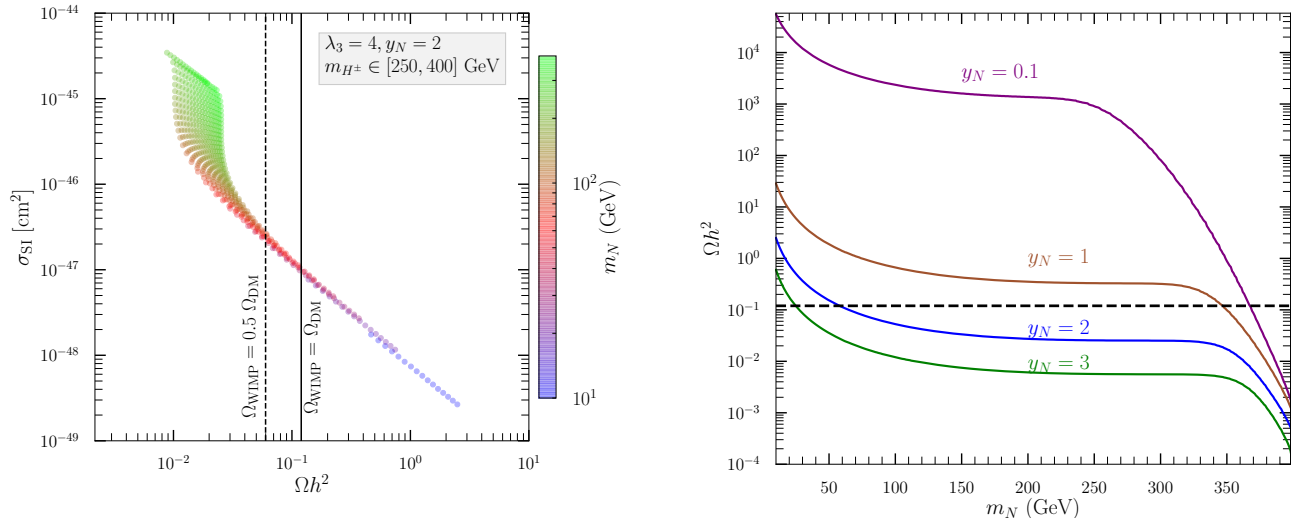


FIG. 2. *Left*: Correlation between the relic density and the spin-independent direct detection cross section. The palette shows the value of the DM mass. The two vertical lines correspond to $\Omega h^2 = \Omega_{\text{Planck}} h^2$ (solid) and $\Omega h^2 = 0.5 \Omega_{\text{Planck}} h^2$ (dashed). *Right*: Dependence of the relic density as a function of the Majorana mass m_N for $m_{H^\pm} = 400$ GeV.

u -channel. The contribution of s -channel diagrams to the relic density is one-loop induced, and therefore is sub-leading, below 1% of the total contribution. Note that the annihilation rate in the s -channel does not depend significantly on λ_3 if this parameter had to satisfy the perturbativity bound. For small mass-splittings, i.e. $\Delta = (m_{H^\pm} - m_N)/m_N < 0.10$, we find that co-annihilations become important and for some values of the model parameters can dominate over the annihilation processes, and hence we include them in our analysis. The scattering of N particles off nuclei occurs at the one-loop level through the exchange of the SM Higgs boson. Hence, the scattering matrix elements $\mathcal{M}(Nq \rightarrow Nq) \propto \mathcal{Y}_{HNN}$ which is given by [31, 32]

$$\mathcal{Y}_{HNN} \simeq -\frac{\lambda_3 v |y_N|^2}{16\pi m_N} \left[1 - (1 - r_N^{-2}) \log(1 - r_N^2) \right], \quad (5)$$

with $r_N = m_N/m_{H^\pm}$. The spin-independent cross section scales as $\lambda_3^2 |y_N|^4 / m_N^2$ modulo factors that depend on mass-splitting between the charged Higgs boson and the Majorana DM. To compute the relic abundance and Spin-independent Nucleus-DM elastic cross sections we use MADDM tool [33]. We find that in order to avoid the over-abundance of DM, the yukawa coupling y_N should not be smaller than 0.1 independent of what value the parameter λ_3 can take (see right panel of Fig. 2). On the other hand, y_N of order $\mathcal{O}(0.1)$ yields an extremely small N -nucleus scattering cross section close to the neutrino-floor for almost all the allowed DM masses except for large values of λ_3 and small mass splittings. In the rest of this Letter, we choose the following benchmark sce-

narios

$$250 \leq m_{H^\pm}/\text{GeV} \leq 400, \quad 10 \leq m_N/\text{GeV} < m_{H^\pm},$$

with $\lambda_3 = 4$, and $y_N = 2$. A strong anti-correlation between Ωh^2 and σ_{SI} can be seen in Fig. 2. We can see that the points in the parameter space yielding $\Omega h^2 \simeq \Omega_{\text{Planck}} h^2$ correspond to DM masses $\simeq 30$ -50 GeV for which the corresponding spin-independent cross section is about 9.52 - $10.21 \times 10^{-48} \text{ cm}^2$ which is below the XENON1T bound [3]. However, as $\Delta = (m_{H^\pm} - m_N)/m_N$ gets smaller, the relic density decreases while still satisfying the XENON1T bound. It is also worth noting that the model is unconstrained from the current indirect detection experiments due to the fact that s -channel annihilation channels are loop induced and mediated by the SM Higgs boson, with the predicted annihilation cross sections $\langle \sigma v \rangle \simeq 10^{-37} \text{ cm}^3/\text{s}$ which is orders of magnitude smaller than the FERMI-LAT bounds [34].

This model give rise to several signatures at colliders. At hadron colliders, the pair production of charged Higgs can occur through the exchange of a photon, and hence its cross section is independent of the model parameters (λ_3 and y_N). However, the corresponding cross section is extremely small; $\sigma_{pp \rightarrow H^+ H^-} = 3.47$ - 0.05 fb for $m_{H^\pm} = 250$ - 400 GeV . This process yields a $2\ell + E_T^{\text{miss}}$ final state, and therefore there is no chance for observing this signal and also due to the large associated background. The process of mono-jet production via the exchange of a SM Higgs boson is highly suppressed as it occurs at the two-loop order. Besides, one can search for

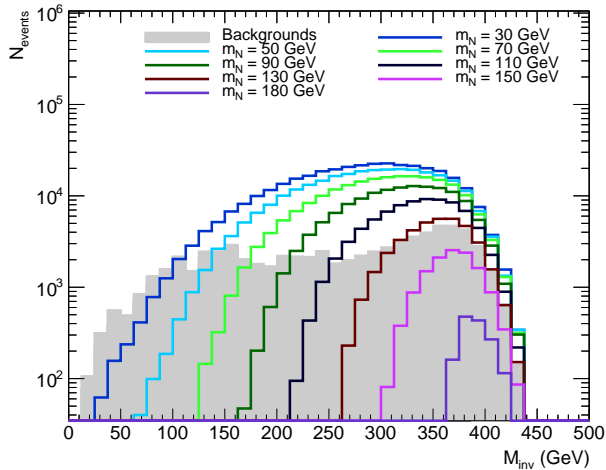


FIG. 3. The expected number of events as function of the invariant mass of the invisible system for the signal and the background. The expected event yield is shown for the total luminosity of $\mathcal{L} = 4000 \text{ fb}^{-1}$. For the signal processes, we have chosen $m_{H^\pm} = 250 \text{ GeV}$, $y_e = 2$ and $\lambda_3 = 4$.

the model signatures at the future International Linear Collider (ILC) which is planned to run at center-of-mass energies of 250, 350, 500, and 1000 GeV [35] and will include the collision of electron beams [36, 37]. The advantage of the latter option is that it can be used efficiently to probe lepton-violating processes due to the negligibly small backgrounds. We consider two signal processes; mono-Higgs process in e^+e^- collisions at $\sqrt{s} = 500 \text{ GeV}$, and same-sign charged Higgs pair production in e^-e^- collisions at 1000 GeV. For the mono-Higgs process, we consider the $H \rightarrow b\bar{b}$ decay channel of the SM Higgs boson for which the major backgrounds are $H(\rightarrow b\bar{b})Z(\rightarrow \nu\bar{\nu})$, $H(\rightarrow b\bar{b})\nu_e\bar{\nu}_e$, W^+W^- , ZZ , and $t\bar{t}$. The last three sources of backgrounds are below the percent level in the signal-like region which we define below. Signal and background processes are generated using MADGRAPH5_AMC@NLO [38] and passed to PYTHIA8 [39] to add parton showering, hadronisation, and hadron decays. We employ DELPHES [40] to add for detector angularity, jet smearing, and particle resolutions. Jets are clustered according to the anti- k_T algorithm [41] with $D = 0.4$ using FASTJET [42]. We select events that pass the following pre-selection criteria

- no lepton (electron or muon) with $p_T^\ell > 15 \text{ GeV}$ and $|\eta^\ell| < 2.5$.
- Exactly two b -tagged jets with $p_T^b > 30 \text{ GeV}$ and $|\eta^b| < 2.5$.

Furthermore, the two b -tagged jets are used to form Higgs boson *candidate* whose transverse momentum is required to be larger than 50 GeV. The invariant mass of the invisible system is related to the energy of the Higgs

boson candidate by the following relation

$$M_{\text{inv}}^2 = s - 2\sqrt{s}E_{b\bar{b}} + M_{b\bar{b}}^2, \quad (6)$$

with \sqrt{s} being the center-of-mass energy, and $E_{b\bar{b}}$ ($M_{b\bar{b}}$) is the energy (the invariant mass) of the $b\bar{b}$ system. We define the signal region by: (1) the invariant mass of the $b\bar{b}$ system is required to satisfy $|M_{b\bar{b}} - m_H| < 10 \text{ GeV}$, and (2) the invariant mass of the invisible system to satisfy $200 \text{ GeV} < M_{\text{inv}} < 400 \text{ GeV}$. In Fig. 3, we show the expected event yields for the signal process (for different DM masses), and the background as a function of the invisible invariant mass.

The charged Higgs pair production in the electron-electron option at the ILC is certainly very interesting. The reasons are two-fold; 1) the signal is enhanced for large DM masses due to the Majorana nature of the DM, and 2) the background is extremely suppressed since the SM processes conserve lepton number. The cross section for the signal behaves as [43]

$$\sigma_{e^-e^- \rightarrow H^-H^-} \propto m_N^2 y_e^4, \quad (7)$$

Considering the decay of the charged Higgs boson into e^-N , the dominant backgrounds are $W^-W^-\nu_e\nu_e$ and Ze^-e^- with the corresponding cross sections 21.53 fb and 98.1 fb respectively. The cross section for the signal processes is orders of magnitude higher; for $m_{H^\pm} = 250 \text{ GeV}$ we have $\sigma_{H^-H^-} = 5.46$ (32.94) pb for $m_N = 30$ (180) GeV. Given the large signal-to-background ratios, we only apply some minor selections on the decay products of the charged Higgs; i.e. two same-sign electrons with $p_T > 20 \text{ GeV}$, and $|\eta| < 2.5$. Using the q_0 -test statistics, we estimate the signal significance for the two processes [44]. In the left panel of Fig. 4, we display the signal significance as a function of the DM mass where we can see that DM masses up to 150 GeV can be probed using the mono-Higgs process. On the other hand, the mono-Higgs process is strongly correlated to the relic density since lighter DM particles give rise to larger relic density and to higher signal significance than for heavier DM. The signal significance for the charged pair production is shown in the right panel of Fig. 4. Contrary to the mono-Higgs process, charged Higgs pair production can probe the whole parameter space of the model even at moderate luminosities. On the other hand, this process can be used to probe regions that are very hard to disentangle by direct detection methods.

In summary, we studied the interesting scenario where DM is a Majorana singlet fermion using simple correlations between the relic abundance and the spin-independent cross sections. We showed that DM masses consistent with the PLANCK observations are still allowed by the XENON1T bound, and well above the neutrino-floor which makes it testable at future direct detection experiments. Besides, we found that this model can be probed at lepton colliders using the mono-Higgs process

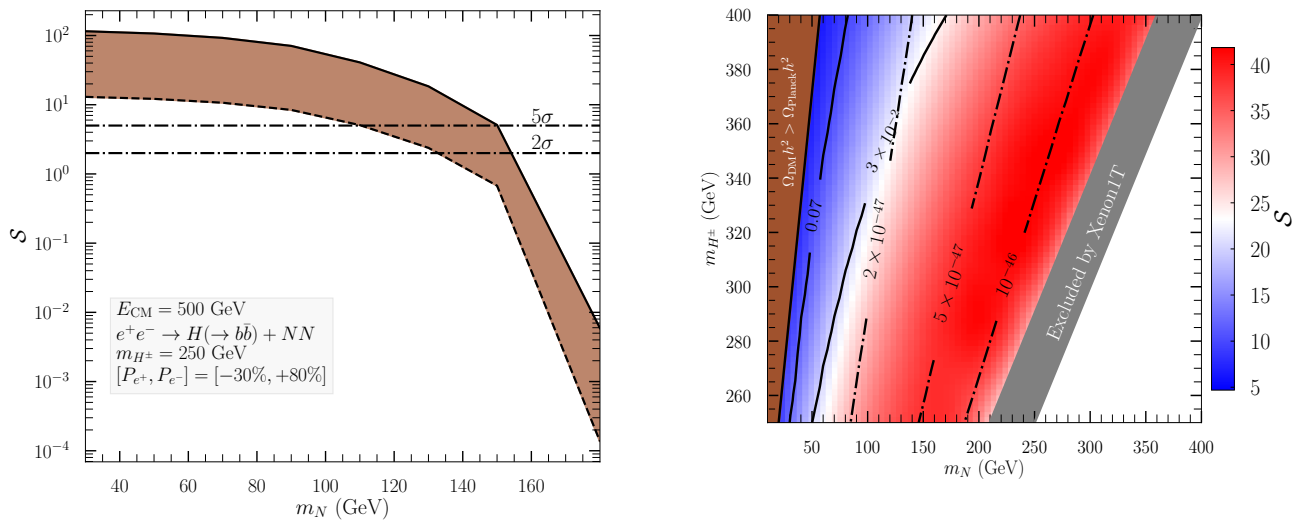


FIG. 4. *Left*: Signal significance as a function of the DM mass in the $e^+e^- \rightarrow H(\rightarrow b\bar{b}) + E_T^{\text{miss}}$ at $\sqrt{s} = 500$ GeV. The solid black shows the significance when only the statistical error is taken into account while the dashed line corresponds to an additional 10% flat systematic uncertainty. *Right*: The signal significance projected on the DM mass and the charged Higgs boson mass for $\mathcal{L} = 10 \text{ fb}^{-1}$. The solid lines show the values of the relic density while the dot-dashed lines show the spin-independent cross sections.

and the same-sign charged Higgs pair production. Important steps are yet to be made regarding the probes of these scenarios using one of the many developed methods to study the characteristics of DM at colliders. One can also obtain the interaction (1) from a more UV complete model. For instance, this can be realized by embedding the SM into $SU(5)$ gauge group with the matter fields in 10 and $\bar{5}$ representation and the charged singlet belongs to the 10_H representation, while the right handed neutrino belongs to the singlet representation, i.e. $\mathcal{L}_{\text{int}} = g_{\alpha\beta} \bar{10}_\alpha \otimes 10_H \otimes 1_{N_\beta} \supset g_{\alpha\beta} \ell_{R\alpha}^T C N_\beta S^+$. Another possibility is the flipped- $SU(5) \times U(1)_X$ grand-unified theory, where the right handed lepton field is singlet of $SU(5)$, and the right handed neutrino is a member of the 10 representation. In this case, the interaction (1) can be obtained from the following effective Lagrangian $\mathcal{L}_{\text{int}} = \frac{h_{\alpha\beta}}{\Lambda} \bar{10}_\alpha \otimes \bar{1}_\beta \otimes 10_H \otimes 1_S + h.c \supset \frac{h_{\alpha\beta} \langle 10_H \rangle}{\Lambda} N^T C \ell_R S^-$. The embedding of our model into a grand-unified theory is certainly an interesting question to pursue which we report on for a future study [45].

AJ would like to thank the CERN Theoretical Physics Department for its hospitality where a part of this work has been done. The work of AJ is supported by the National Research Foundation of Korea, Grant No. NRF-2019R1A2C1009419.

* adiljueid@konkuk.ac.kr

† salah.nasri@gmail.com

- [1] G. Bertone, D. Hooper, and J. Silk, Phys. Rept. **405**, 279 (2005), hep-ph/0404175.
- [2] P. A. R. Ade et al. (Planck), Astron. Astrophys. **594**, A13 (2016), 1502.01589.
- [3] E. Aprile et al. (XENON), Phys. Rev. Lett. **121**, 111302 (2018), 1805.12562.
- [4] X. Cui et al. (PandaX-II), Phys. Rev. Lett. **119**, 181302 (2017), 1708.06917.
- [5] O. Adriani et al. (PAMELA), Phys. Rev. Lett. **105**, 121101 (2010), 1007.0821.
- [6] M. Aguilar et al. (AMS), Phys. Rev. Lett. **110**, 141102 (2013).
- [7] M. Ahnen et al. (MAGIC, Fermi-LAT), JCAP **02**, 039 (2016), 1601.06590.
- [8] H. Abdallah et al. (H.E.S.S.), Phys. Rev. Lett. **117**, 111301 (2016), 1607.08142.
- [9] B. Meirose (ATLAS), Int. J. Mod. Phys. Conf. Ser. **43**, 1660196 (2016).
- [10] S. Ahuja (CMS), PoS **LHCP2018**, 284 (2018).
- [11] R. K. Leane, T. R. Slatyer, J. F. Beacom, and K. C. Y. Ng, Phys. Rev. **D98**, 023016 (2018), 1805.10305.
- [12] V. Silveira and A. Zee, Phys. Lett. B **161**, 136 (1985).
- [13] C. Burgess, M. Pospelov, and T. ter Veldhuis, Nucl. Phys. B **619**, 709 (2001), hep-ph/0011335.
- [14] G. Arcadi, C. Gross, O. Lebedev, S. Pokorski, and T. Toma, Phys. Lett. B **769**, 129 (2017), 1611.09675.
- [15] J. A. Casas, D. G. Cerdeo, J. M. Moreno, and J. Quilis, JHEP **05**, 036 (2017), 1701.08134.

- [16] L. M. Krauss, S. Nasri, and M. Trodden, *Phys. Rev. D* **67**, 085002 (2003), hep-ph/0210389.
- [17] Y. Cai, J. Herrero-Garcia, M. A. Schmidt, A. Vicente, and R. R. Volkas, *Front. in Phys.* **5**, 63 (2017), 1706.08524.
- [18] M. Aoki, S. Kanemura, and O. Seto, *Phys. Rev. Lett.* **102**, 051805 (2009), 0807.0361.
- [19] B. Swiezewska and M. Krawczyk, *Phys. Rev. D* **88**, 035019 (2013), 1212.4100.
- [20] G. Aad et al. (ATLAS, CMS), *JHEP* **08**, 045 (2016), 1606.02266.
- [21] G. C. Branco, P. M. Ferreira, L. Lavoura, M. N. Rebelo, M. Sher, and J. P. Silva, *Phys. Rept.* **516**, 1 (2012), 1106.0034.
- [22] S. Kanemura, T. Kubota, and E. Takasugi, *Phys. Lett.* **B313**, 155 (1993), hep-ph/9303263.
- [23] I. F. Ginzburg, K. A. Kanishev, M. Krawczyk, and D. Sokolowska, *Phys. Rev.* **D82**, 123533 (2010), 1009.4593.
- [24] T. Hahn, *Nucl. Phys. Proc. Suppl.* **89**, 231 (2000), hep-ph/0005029.
- [25] T. Hahn, *Comput. Phys. Commun.* **140**, 418 (2001), hep-ph/0012260.
- [26] A. M. Sirunyan et al. (CMS), *Phys. Lett. B* **793**, 520 (2019), 1809.05937.
- [27] G. Passarino and M. Veltman, *Nucl. Phys. B* **160**, 151 (1979).
- [28] J. Adam et al. (MEG), *Phys. Rev. Lett.* **110**, 201801 (2013), 1303.0754.
- [29] B. Aubert et al. (BaBar), *Phys. Rev. Lett.* **104**, 021802 (2010), 0908.2381.
- [30] T. Toma and A. Vicente, *JHEP* **01**, 160 (2014), 1312.2840.
- [31] A. Ahriche, A. Jueid, and S. Nasri, *Phys. Rev.* **D97**, 095012 (2018), 1710.03824.
- [32] N. Okada and T. Yamada, *JHEP* **10**, 017 (2013), 1304.2962.
- [33] F. Ambrogio, C. Arina, M. Backovic, J. Heisig, F. Maltoni, L. Mantani, O. Mattelaer, and G. Mohlabeng, *Phys. Dark Univ.* **24**, 100249 (2019), 1804.00044.
- [34] M. Ackermann et al. (Fermi-LAT), *Phys. Rev. D* **91**, 122002 (2015), 1506.00013.
- [35] H. Baer, T. Barklow, K. Fujii, Y. Gao, A. Hoang, S. Kanemura, J. List, H. E. Logan, A. Nomerotski, M. Perelstein, et al. (2013), 1306.6352.
- [36] J. L. Feng, *Int. J. Mod. Phys.* **A15**, 2355 (2000), hep-ph/0002055.
- [37] C. A. Heusch, *Int. J. Mod. Phys.* **A20**, 7289 (2005).
- [38] J. Alwall, R. Frederix, S. Frixione, V. Hirschi, F. Maltoni, O. Mattelaer, H. S. Shao, T. Stelzer, P. Torrielli, and M. Zaro, *JHEP* **07**, 079 (2014), 1405.0301.
- [39] T. Sjöstrand, S. Ask, J. R. Christiansen, R. Corke, N. Desai, P. Ilten, S. Mrenna, S. Prestel, C. O. Rasmussen, and P. Z. Skands, *Comput. Phys. Commun.* **191**, 159 (2015), 1410.3012.
- [40] J. de Favereau, C. Delaere, P. Demin, A. Giammanco, V. Lematre, A. Mertens, and M. Selvaggi (DELPHES 3), *JHEP* **02**, 057 (2014), 1307.6346.
- [41] M. Cacciari, G. P. Salam, and G. Soyez, *JHEP* **04**, 063 (2008), 0802.1189.
- [42] M. Cacciari, G. P. Salam, and G. Soyez, *Eur. Phys. J.* **C72**, 1896 (2012), 1111.6097.
- [43] M. Aoki and S. Kanemura, *Phys. Lett. B* **689**, 28 (2010), 1001.0092.
- [44] G. Cowan, K. Cranmer, E. Gross, and O. Vitells, *Eur. Phys. J.* **C71**, 1554 (2011), [Erratum: *Eur. Phys. J.* **C73**, 2501(2013)], 1007.1727.
- [45] A. Jueid and S. Nasri, To be published (2020).